

# Dimer models for parallelograms

Kazushi Ueda and Masahito Yamazaki

## Abstract

We discuss the relation between dimer models and coamoebas associated with lattice parallelograms. We also discuss homological mirror symmetry for  $\mathbb{P}^1 \times \mathbb{P}^1$ , emphasizing the role of a non-isoradial dimer model.

## 1 Introduction

This is a short companion paper to [8, 9], where we discuss the relation between dimer models, coamoebas and homological mirror symmetry, following the work of string theorists [1, 2, 3, 4, 5, 6]. We refer the readers to [8, 9] and references therein for notations and backgrounds. We show the following in this paper:

- The linear Hanany-Vegh algorithm produces a unique dimer model from a lattice parallelogram.
- For a suitable choice of a Laurent polynomial  $W$ , the zero locus  $W^{-1}(0)$  behaves nicely under the argument map  $\text{Arg} : (\mathbb{C}^\times)^2 \rightarrow (\mathbb{R}/\mathbb{Z})^2$ .
- The dimer model is the argument projection of a graph on  $W^{-1}(0)$ , which encodes Floer-theoretic information of vanishing cycles.

As a corollary, one obtains a torus-equivariant generalization of homological mirror symmetry for  $\mathbb{P}^1 \times \mathbb{P}^1$  proved by Seidel [7]. We also discuss the role of a non-isoradial dimer model which cannot be obtained by the linear Hanany-Vegh algorithm.

## 2 Coamoebas for lattice parallelograms

We prove the following in this section:

**Theorem 2.1.** *For any lattice parallelogram, there exists a Laurent polynomial  $W$  satisfying the following:*

- *The Newton polygon of  $W$  coincides with the lattice parallelogram.*
- *The set  $\mathcal{A}$  of asymptotic boundaries of the coamoeba of  $W^{-1}(0)$  is the unique admissible arrangement of oriented lines associated with the lattice parallelogram.*
- *The coamoeba is the union of colored cells and vertices of  $\mathcal{A}$ .*

- The restriction of the argument map to the inverse image of a colored cell is a diffeomorphism. It is orientation-preserving if the cell is white, and reversing if the cell is black.
- The inverse image of a vertex of  $\mathcal{A}$  by the argument map is homeomorphic to an open interval.

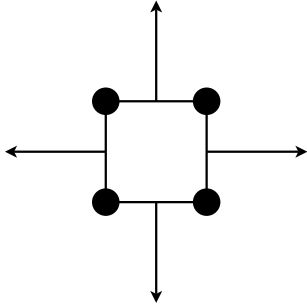


Figure 2.1: A lattice square

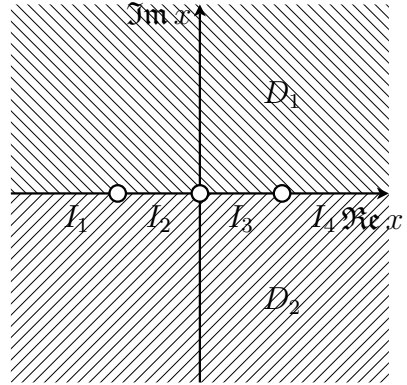


Figure 2.2: The projection of  $W^{-1}(0)$  to the  $x$ -plane

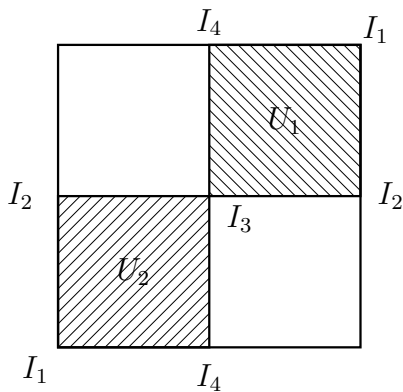


Figure 2.3: The coamoeba

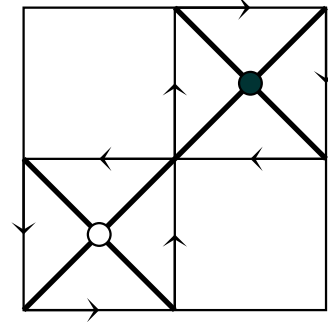


Figure 2.4: The dimer model

*Proof.* Since any lattice parallelogram is obtained from the convex hull of  $(0, 0)$ ,  $(0, 1)$ ,  $(1, 0)$  and  $(1, 1)$  shown in Figure 2.1 by a translation and an integral linear transformation, it suffices to discuss the case

$$W(x, y) = xy + x - y + 1.$$

The projection

$$\begin{array}{ccc} W^{-1}(0) & \rightarrow & \mathbb{C}^\times \\ \cup & & \cup \\ (x, y) & \mapsto & x \end{array}$$

to the  $x$ -plane is injective, whose image is obtained by gluing the upper half plane

$$D_1 = \{x \in \mathbb{C} \mid \Im(x) > 0\}$$

and the lower half plane

$$D_2 = \{x \in \mathbb{C} \mid \Im(x) < 0\}$$

along four intervals

$$I_1 = (-\infty, -1), I_2 = (-1, 0), I_3 = (0, 1), \text{ and } I_4 = (1, \infty).$$

as shown in Figure 2.2. Set

$$U_1 = \left\{ (\theta, \phi) \in T \mid 0 < \theta < \frac{1}{2}, 0 < \phi < \frac{1}{2} \right\},$$

$$U_2 = \left\{ (\theta, \phi) \in T \mid -\frac{1}{2} < \theta < 0, -\frac{1}{2} < \phi < 0, \right\}.$$

Then the argument map gives an orientation-reversing homeomorphism from  $D_1$  to  $U_1$  and an orientation-preserving homeomorphism from  $D_2$  to  $U_2$ . The line segments  $I_1, I_2, I_3$  and  $I_4$  on the boundary of  $D_1$  and  $D_2$  are mapped to four points  $(\frac{1}{2}, \frac{1}{2}), (\frac{1}{2}, 0), (0, 0)$  and  $(0, \frac{1}{2})$  respectively. This shows that the coamoeba of  $W^{-1}(0)$  is as in Figure 2.3. Its asymptotic boundaries and the corresponding dimer model is shown in Figure 2.4.

The uniqueness of the output of the linear Hanany-Vegh algorithm can be shown in just the same way as the case of triangles in [8, Section 5.6], and we omit the detail here.  $\square$

### 3 Vanishing cycles for the mirror of $\mathbb{P}^1 \times \mathbb{P}^1$

We prove [9, Conjecture 6.2] for  $\mathbb{P}^1 \times \mathbb{P}^1$  in this section. The mirror of  $\mathbb{P}^1 \times \mathbb{P}^1$  is given by the Laurent polynomial

$$W(x, y) = x - \frac{1}{x} + y + \frac{1}{y},$$

whose critical points are given by

$$(x, y) = (-\sqrt{-1}, -1), (\sqrt{-1}, -1), (\sqrt{-1}, 1), (-\sqrt{-1}, 1),$$

with critical values

$$(p_1, p_2, p_3, p_4) = (-2 - 2\sqrt{-1}, -2 + 2\sqrt{-1}, 2 + 2\sqrt{-1}, 2 - 2\sqrt{-1}).$$

Let  $(c_i)_{i=1}^4$  be a distinguished set of vanishing paths, obtained as the straight line segments from the origin to the critical values of  $W$  as shown in Figure 3.1. The fiber of  $W$  can be realized as a branched cover of  $\mathbb{C}$  by

$$\begin{array}{ccc} \pi_t : W^{-1}(t) & \rightarrow & \mathbb{C} \\ \cup & & \cup \\ (x, y) & \mapsto & x - \frac{1}{x} \end{array}$$

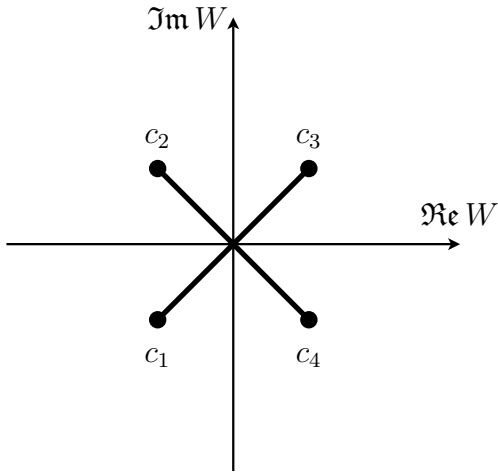


Figure 3.1: A distinguished set of vanishing paths

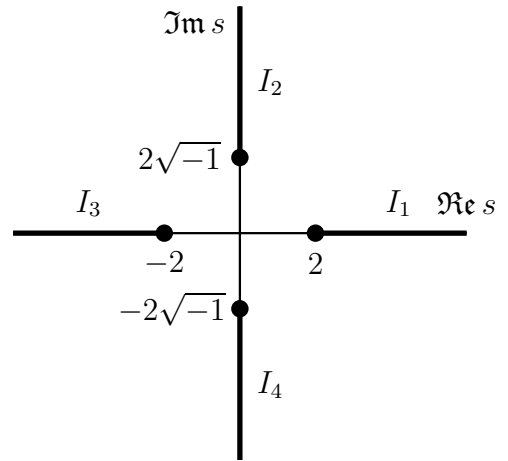


Figure 3.2: Branch points and cuts on the  $s$ -plane

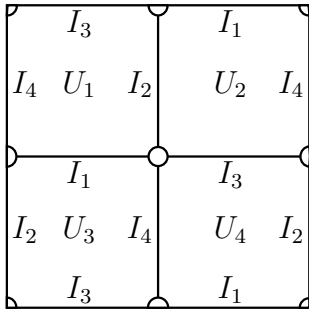


Figure 3.3: The glued surface  $W^{-1}(0)$

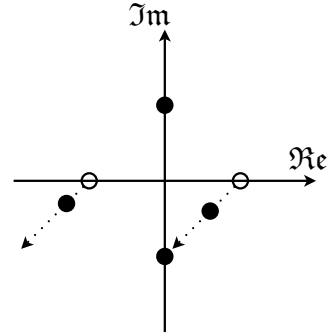


Figure 3.4: Behavior of the branch points along  $c_1$

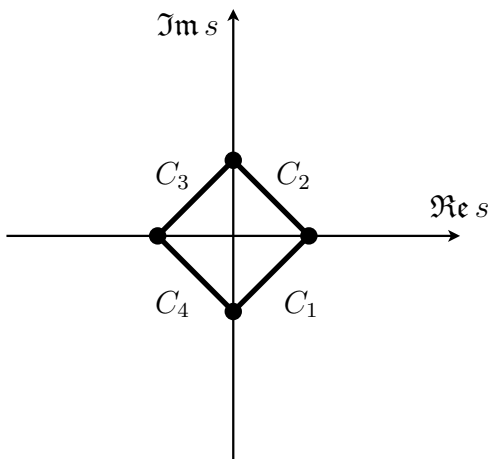


Figure 3.5: The images of four vanishing cycles on the  $s$ -plane

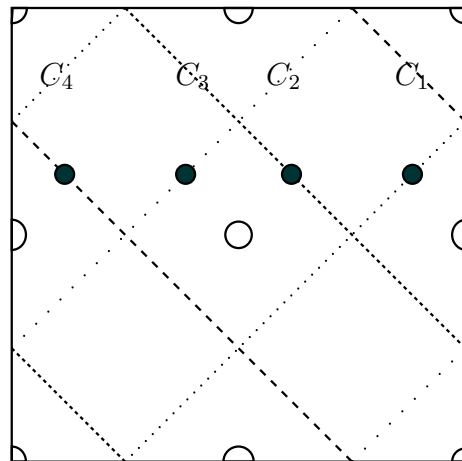


Figure 3.6: Vanishing cycles on  $W^{-1}(0)$

for  $t \in \mathbb{C}$ . The fiber of  $\pi_t$  at a general point  $s \in \mathbb{C}$  consists of four points, which is the product of the set of solutions of

$$x - \frac{1}{x} = s \tag{3.1}$$

with that of

$$y + \frac{1}{y} = t - s. \tag{3.2}$$

The set of solutions of (3.1) degenerates at  $s = \pm 2\sqrt{-1}$ , whereas that of (3.2) degenerates at  $s = \pm 2 + t$ . The fiber  $W^{-1}(0)$  is obtained by gluing four copies  $U_1, \dots, U_4$  of the  $s$ -plane cut along four half lines  $I_1, \dots, I_4$  as in Figure 3.2. The resulting surface is shown in Figure 3.3.

Two of the four branch points of  $\pi_t$  move as in Figure 3.4 as one varies  $t$  from 0 to  $p_1 = -2 - 2\sqrt{-1}$  along  $c_1$ . This shows that the image by  $\pi_0$  of the corresponding vanishing cycle  $C_1$  is the line segment from 2 to  $-2\sqrt{-1}$  up to homotopy. Figure 3.5 shows four line segments on the  $s$ -plane, which are images of the vanishing cycles of  $W$  shown in Figure 3.6. One can equip these vanishing cycles with gradings so that the Maslov indices of the intersection points in  $C_1 \cap C_2$ ,  $C_2 \cap C_3$ , and  $C_3 \cap C_4$  are 1. Then the Maslov indices of intersection points in  $C_1 \cap C_4$  are 2. The dot in Figure 3.6 shows our choice of branch points for the non-trivial spin structures.

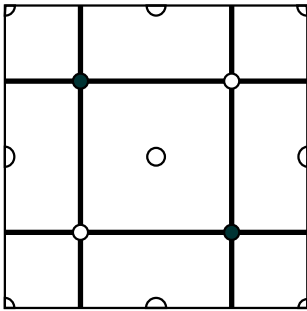


Figure 3.7: The graph on  $W^{-1}(0)$

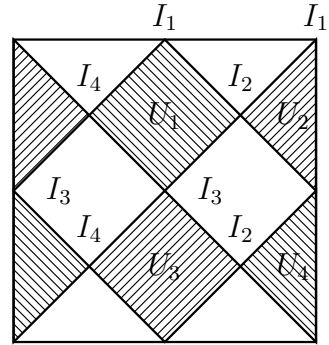


Figure 3.8: The coamoeba

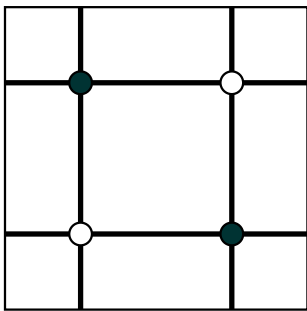


Figure 3.9: The dimer model  $G$

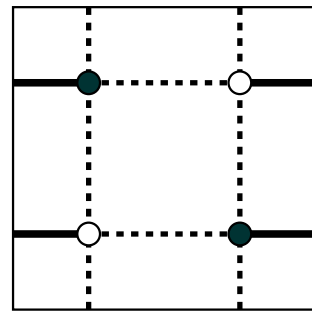


Figure 3.10: The perfect matching  $D$

There are four quadrangles in  $W^{-1}(0)$  bounded by  $\bigcup_{i=1}^4 C_i$ , which correspond to  $A_\infty$ -operations in  $\mathfrak{Fuk}W$ . By contracting these quadrangles, one obtains the bicolored graph in Figure 3.7. Figure 3.8 shows the coamoeba of  $W^{-1}(0)$ , and Figure 3.9 shows the dimer model  $G$ . Here, the black node on the top left in Figure 3.9 corresponds to  $U_1$  in Figure 3.8.

The perfect matching  $D$  coming from the order in the distinguished basis of vanishing cycles is shown in Figure 3.10. The full strong exceptional collection of line bundles on  $\mathbb{P}^1 \times \mathbb{P}^1$  associated with the pair  $(G, D)$  is given by

$$(E_1, E_2, E_3, E_4) = (\mathcal{O}, \mathcal{O}(1, 0), \mathcal{O}(1, 1), \mathcal{O}(2, 1)), \quad (3.3)$$

where  $\mathcal{O}(i, j) = \mathcal{O}_{\mathbb{P}^1}(i) \boxtimes \mathcal{O}_{\mathbb{P}^1}(j)$  denotes the exterior tensor product of the  $i$ -th and  $j$ -th tensor powers of the hyperplane bundle on  $\mathbb{P}^1$  for  $i, j \in \mathbb{Z}$ .

## 4 Non-isoradial dimer model and vanishing cycles

In this section, we discuss the role of the non-isoradial dimer model in Figure 4.16 below, which corresponds to the full strong exceptional collection

$$(E_1, E_2, E_3, E_4) = (\mathcal{O}, \mathcal{O}(1, 0), \mathcal{O}(0, 1), \mathcal{O}(1, 1)) \quad (4.1)$$

of line bundles on  $\mathbb{P}^1 \times \mathbb{P}^1$ . This collection is obtained from the collection (3.3) by the right mutation at the last term, and the corresponding vanishing paths are shown in Figure 4.1. Figure 4.2 shows the images of vanishing cycles by the projection to the  $s$ -plane. The vanishing cycles on  $W^{-1}(0)$  are shown in Figure 4.3, and by contracting eight triangles bounded by them, one obtains the bicolored graph on  $W^{-1}(0)$  shown in Figure 4.4.

Unfortunately, the argument projection of this graph does not give a dimer model. Figure 4.5 shows the image of this graph on the  $s$ -plane. Here, two white dots are images of eight nodes, and four black dots are branch points where the fiber becomes two points instead of four points.

Consider the deformation

$$W_t(x, y) = x + \frac{2t-1}{x} + y + \frac{t+1}{y}$$

from

$$W_0(x, y) = x - \frac{1}{x} + y + \frac{1}{y}$$

to

$$W_1(x, y) = x + \frac{1}{x} + y + \frac{2}{y}.$$

Figure 4.6 shows the behavior of the branch points under this deformation. The graph in Figure 4.5 is deformed to the graph in Figure 4.7. We put labels on this graph as in Figure 4.8.

Note that the map

$$\begin{array}{ccc} \mathbb{C}^\times & \rightarrow & \mathbb{C} \\ \cup & & \cup \\ x & \mapsto & x + \frac{1}{x} \end{array}$$

from the  $x$ -plane to the  $s$ -plane is a branched double cover, which maps both the upper half plane and the lower half plane into the whole  $s$ -plane minus

$$I = I_+ \amalg I_- = \{s \in \mathbb{R} \mid |s| \geq 2\},$$

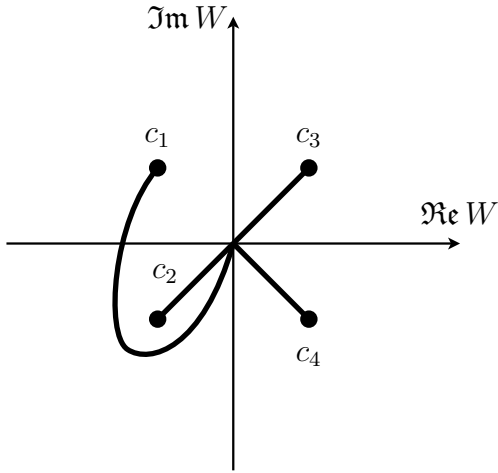


Figure 4.1: A distinguished set of vanishing paths

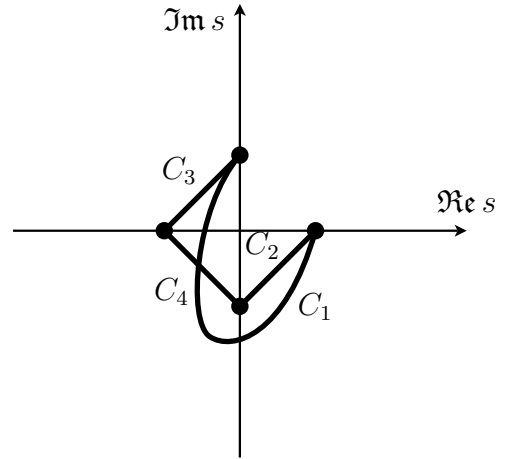


Figure 4.2: Images of vanishing cycles

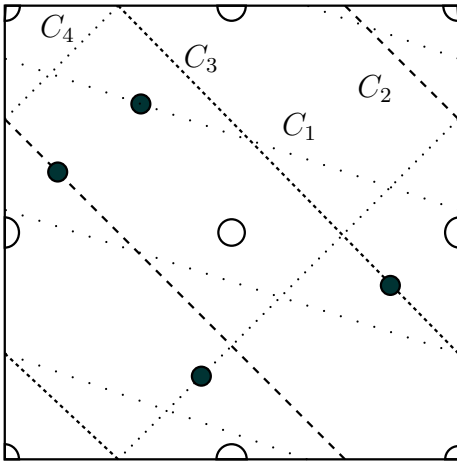


Figure 4.3: Vanishing cycles on  $W^{-1}(0)$

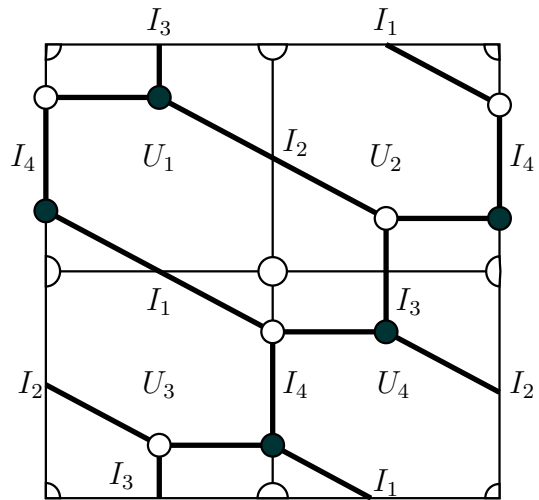


Figure 4.4: The graph on  $W^{-1}(0)$

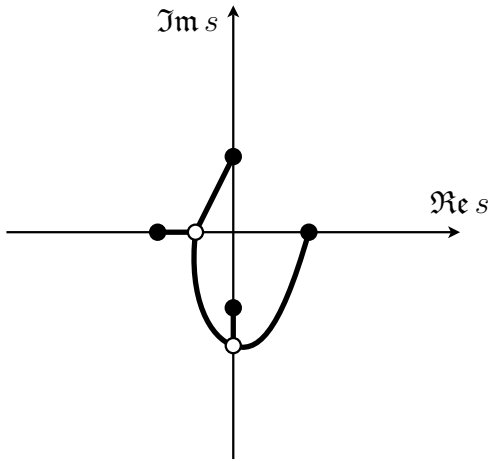


Figure 4.5: The image of the graph on the  $s$ -plane

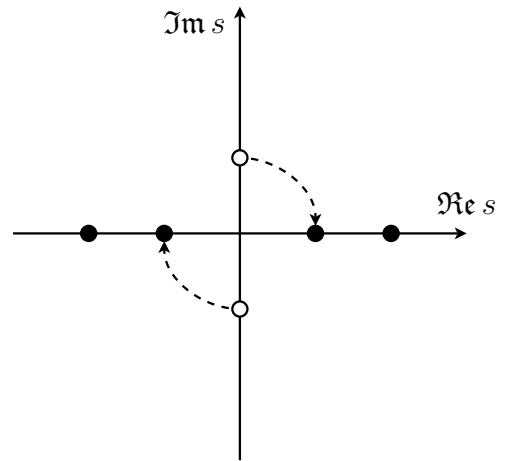


Figure 4.6: Behavior of the branch points

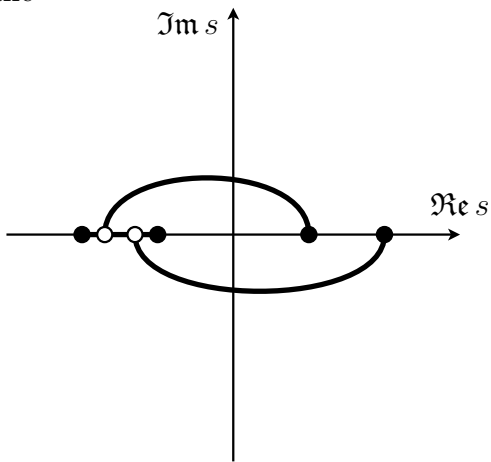


Figure 4.7: The deformed graph

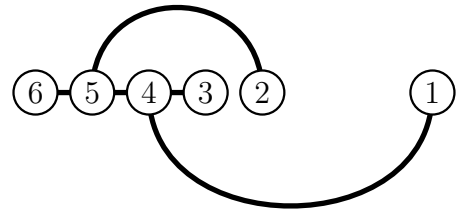


Figure 4.8: Labels on the graph on the  $s$ -plane





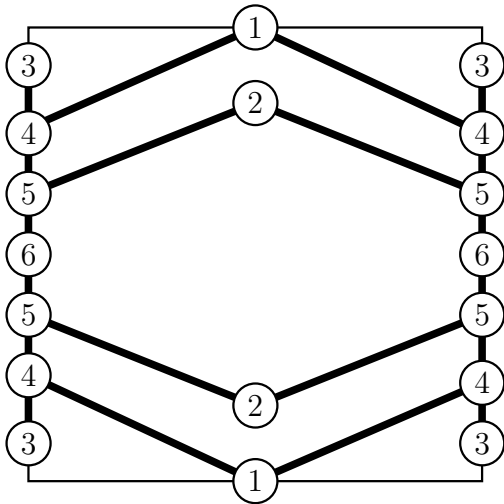


Figure 4.13: The graph on the torus

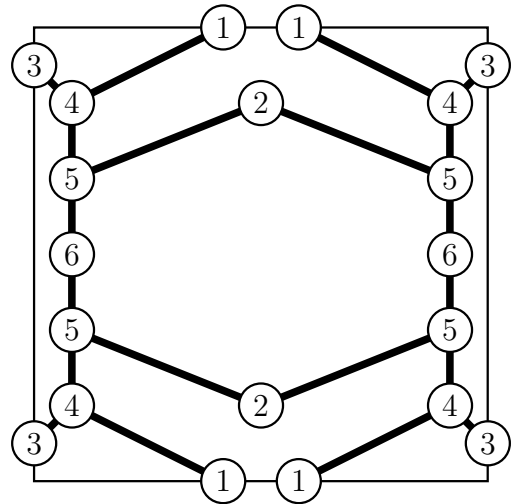


Figure 4.14: A perturbed graph

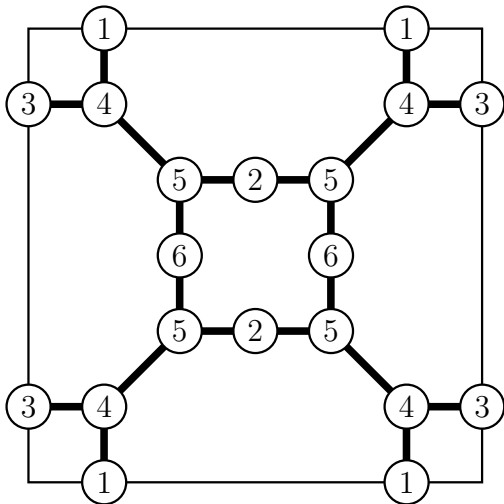


Figure 4.15: A deformed graph

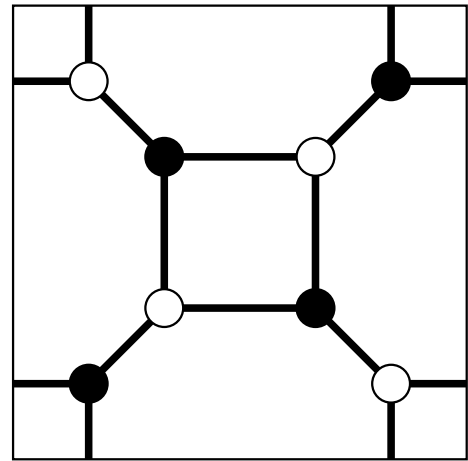


Figure 4.16: The non-isoradial dimer model

## References

- [1] Bo Feng, Yang-Hui He, Kristian D. Kennaway, and Cumrun Vafa. Dimer models from mirror symmetry and quivering amoebae. *Adv. Theor. Math. Phys.*, 12(3):489–545, 2008.
- [2] Sebastián Franco, Amihay Hanany, Dario Martelli, James Sparks, David Vegh, and Brian Wecht. Gauge theories from toric geometry and brane tilings. *J. High Energy Phys.*, (1):128, 40 pp. (electronic), 2006.
- [3] Sebastián Franco, Amihay Hanany, David Vegh, Brian Wecht, and Kristian D. Kennaway. Brane dimers and quiver gauge theories. *J. High Energy Phys.*, (1):096, 48 pp. (electronic), 2006.
- [4] Amihay Hanany, Christopher P. Herzog, and David Vegh. Brane tilings and exceptional collections. *J. High Energy Phys.*, (7):001, 44 pp. (electronic), 2006.
- [5] Amihay Hanany and Kristian D. Kennaway. Dimer models and toric diagrams. hep-th/0503149, 2005.
- [6] Amihay Hanany and David Vegh. Quivers, tilings, branes and rhombi. *J. High Energy Phys.*, (10):029, 35, 2007.
- [7] Paul Seidel. More about vanishing cycles and mutation. In *Symplectic geometry and mirror symmetry (Seoul, 2000)*, pages 429–465. World Sci. Publishing, River Edge, NJ, 2001.
- [8] Kazushi Ueda and Masahito Yamazaki. A note on dimer models and McKay quivers. math.AG/0605780.
- [9] Kazushi Ueda and Masahito Yamazaki. Homological mirror symmetry for toric orbifolds of toric del Pezzo surfaces. math.AG/0703267.

Kazushi Ueda

Department of Mathematics, Graduate School of Science, Osaka University, Machikaneyama 1-1, Toyonaka, Osaka, 560-0043, Japan.

*e-mail address* : kazushi@math.sci.osaka-u.ac.jp

Masahito Yamazaki

Department of Physics, Graduate School of Science, University of Tokyo, Hongo 7-3-1, Bunkyo-ku, Tokyo, 113-0033, Japan

*e-mail address* : yamazaki@hep-th.phys.s.u-tokyo.ac.jp